Evolution of Fragment Distributions and Reaction Mechanisms for the Ar+Ni System from 32 to 95 A.MeV

Laurent Nalpas, J.L. Charvet, R. Dayras, E. de Filippo, G. Auger, Ch.O. Bacri, A. Benkirane, J. Benlliure, B. Berthier, B. Borderie, et al.

Evolution of Fragment Distributions and Reaction Mechanisms for the ^{36}Ar+^{58}Ni System from 32 to 95 A.MeV.

L. Nalpas[1] J.L. Charvet[1], R. Dayras[1], E. De Filippo[1], G. Auger[3], Ch.O. Bacri[2], A. Benkirane[3], J. Benlliure[3], B. Berthier[1], B. Borderie[2], R. Bougault[4], P. Box[2], R. Brou[4], Y. Cassagnou[1], A. Chbihi[3], J. Colin[4], D. Cussol[4], A. Demeyer[5], D. Durand[4], P. Ecomard[3], P. Eudes[6], A. Genoux-Lubain[4], D. Gourio[6], D. Guinet[5], L. Lakehal-Ayat[2], P. Lautesse[5], P. Lautridou[6], J.L. Laville[6], L. Lebreton[5], C. Le Brun[4], J.F. Lecolley[4], A. Le Fèvre[3], R. Legrain[1], O. Lopez[4], M. Louvel[4], N. Marie[3], V. Métivier[4], T. Nakagawa[4], A. Ouatizerga[2], M. Parlog[2], J. Péter[4], E. Plagnol[2], E.C. Pollacco[1], J. Pouthas[3], A. Rahmani[6], R. Regimbart[4], M.F. Rivet[2], T. Reposeur[6], E. Rosato[4], F. Saint-Laurent[3], M. Squalli[2], J.C. Steckmeyer[4], B. Tamain[4], L. Tassan-Got[2], E. Vient[4], C. Volant[1], J.P. Wieleczko[3], A. Wieloch[4], K. Yuasa Nakagawa[4].

June 24, 2005

(1) DAPNIA/SPhN, CEA Saclay, 91191 Gif/Yvette, France
(2) IPN Orsay, CNRS-Université, 91406 Orsay, France
(3) GANIL, B.P.5027, 14021 Caen, France
(4) LPC Caen, CNRS-ISMRA, 14050 Caen, France
(5) IPN Lyon, CNRS-Université, 69622 Villeurbanne, France
(6) SUBATECH, CNRS-Université, 44072 Nantes, France

Abstract

Within the framework of flow and multifragmentation study, the ^{36}Ar+^{58}Ni experiment has been performed at seven incident energies from 32 to 95 A.MeV with the INDRA detector at GANIL. After a brief description of the experimental set-up, the main trends as well as the evolution of fragment distributions will be presented. Some results about reaction mechanisms for particular classes of events will conclude this report.

1 Introduction

The study of the limiting temperature of hot nuclei has been a major theme of research at intermediate energies for the past decade [1]. At low excitation energy, nuclei usually disintegrate by emitting neutrons and light charged particles (Z=1 and Z=2). When increasing excitation energy, an emission of intermediate mass fragments (IMF namely Z$\geq$3) has been experimentally observed [2]. However up to now the fragment emission mechanism remains poorly understood. Indeed this emission could be described either in continuity of the statistical evaporation process at high excitation energy, or as a multifragmentation process for which fragments are emitted almost simultaneously. Some theoretical calculations support this new interpretation and predict an initial compression phase of the nuclear matter followed by an expansion phase during which the fragments are created [3, 4]. Moreover a liquid-gaz phase transition could be associated with this multifragmentation process [5]. The new generation of 4π detector such as INDRA should give some reliable answers to these open questions in the next years.

2 Experimental set-up

The INDRA detector is dedicated to the measurement of the charge and of the kinematical properties of light particles and fragments. The overall characteristics of the detector and of its electronics as well as the identification and calibration methods are presented in details in Ref. [6]. In few words, the detector is composed of 336 detection modules over 17 rings covering 90% of 4π. The first ring (2°-3°) is made of 12 plastic scintillator phoswiches (NE102/NE115) able to endure high counting rates. The forward rings (3°-45°) are made of three-stage telescopes composed of a low pressure ionization chamber followed by a wafer of three or four 300 μm thick silicon detectors, each followed by a CsI(Tl) scintillator stopping all fast products. For the backward rings (45°-176°) the silicon detectors are removed due to the smaller velocity range of the fragments.

Such a set-up provides high granularity and geometrical efficiency as well as a large energy range with low detection thresholds for light particles and fragments in order to study high multiplicity events coming from the de-excitation of hot nuclei. The charge identification is performed by the well known ΔE/E technique up to Z$\sim$25 for the slow products and up to Z$\sim$50 for the fastest ones. A shape discrimination method for CsI signals allows an isotopic separation for light charged particles up to Z=4.

For the Ar+Ni experiment performed in 1993, a large range of bombarding energies from 95 to 32 A.MeV was obtained by slowing down the beam through a thick ^{12}C target placed before a magnetic analysis. The multiple interaction rate was kept below 10^{-4} by means of a low ^{36}Ar beam intensity ($\sim$2-3 10^7 particles/sec) as well as a thin ^{58}Ni target (193 μg/cm^2). The data acquisition was activated only

when at least 3 modules were hit for low incident energies (4 hits for the highest). In these conditions, the acquisition dead time was around 20%. For this experiment, the rings beyond 92° were not equipped with ionization chambers. Therefore only identification of light charged particles is possible at backward angles. Moreover the energy calibration for fragments are not available beyond 45° at the present time.

3 General trends

The total detected charge (Z_{TOT}) versus the charged particle multiplicity, plotted in Fig.1, shows an overview of the INDRA efficiency. Indeed the total charge of the system (Z_0=46) is well reconstructed for a large multiplicity range. However, at low multiplicity, two classes of badly detected events corresponding to peripheral collisions can be found. Firstly, at low Z_{TOT}, the projectile-like fragment (PLF) emitted at small angles as well as the low energy target-like fragment (TLF) are not detected owing to the geometrical inefficiency at forward angles on the one hand and the detection thresholds on the other hand. For Z_{TOT} ∼18, the PLF is detected but the TLF is still missing due to the thresholds. In the following only complete events for which Z_{TOT} is greater than 80% of the total charge of the system ($Z_{TOT} \geq$38) are taken into account. This cut-off eliminates about 80% of the events at 32 A.MeV and close to 90% at 95 A.MeV. However a large range of impact parameter is selected as some results about reaction mechanisms will confirm.

The IMF distributions shown in Fig.2a exhibit the same bell shape with a maximum obtained for 2 and 3-IMF events at any bombarding energy. Fig.2b displays the evolution of the relative proportion of events with different IMF multiplicities as a function of the incident energy. The partitions are very similar for all incident energies. The lack of a large variation of the IMF number is an intriguing result which means that the IMF multiplicity is independent of the available energy in the center of mass system. Otherwise minor fluctuations show the existence of a transition around 52 A.MeV in the IMF yield. Indeed from 32 to 52 A.MeV the proportions of 1 and 2-IMF events decrease slightly whereas the other partitions increase. This rise of the IMF yield with energy is predicted by statistical models [5, 7]. However owing to the total charge conservation, the IMF charge falls as the IMF multiplicity goes up. Therefore the high IMF multiplicities reach a maximum around 52 A.MeV. Beyond this energy, a fraction of fragments disappears in light particles (generally Z=2) leading to a steady fall of the high IMF partitions to the benefit of the low IMF multiplicity events. The most striking trend is obtained for the no IMF ratio which increases significantly from 52 to 95 A.MeV expressing the trend towards the vaporization of the nuclear system [8].

4 Evolution of reaction mechanisms

An efficient detector such as INDRA allows to reconstruct event by event the kinematics of the collision and to obtain some information about the reaction mechanisms. In central collisions, at low energies, the fusion process is generally involved in the formation of hot nuclei (at least for the light systems). This process is characterized by the presence of a source close to the center of mass rapidity in Lorentz invariant cross section $\frac{\partial^2\sigma}{\partial y \partial p_\perp}$ plot. However some results have shown that binary processes become dominant with increasing energy [9]. They are characterized by two sources at low rapidity on the one hand and near the projectile rapidity on the other hand. The partition of the total cross section between these reaction mechanisms remains an open question which is linked to the problem of source characterization. Some qualitative results for the particular classes of events including 1 and 2-IMF are now presented.

A relationship between the total multiplicity and an estimated impact parameter has been used to select the most dissipative collisions from the less dissipative ones by means of three multiplicity slices (Fig.3). For the following analysis, only the two extreme mutiplicity slices are considered. The Lorentz invariant cross section plot for alpha particles associated to the 1-IMF events is displayed at 32 A.MeV in Fig.4a. A source can be distinguished around the center of mass rapidity. The IMF velocity and charge distributions confirm the assumption of a fusion process (Fig.4b). Indeed the remaining IMF is relatively heavy and slow ($\langle V \rangle \sim$2 cm/ns close to the detection threshold). Moreover the IMF angular distribution is peaked at forward angle. These overall characteristics are compatible with an incomplete fusion process leading to an evaporation residue with 60% of transferred momentum [10]. The cross section for fusion is estimated at 70 mbarn (2% of the reaction cross section).

When increasing energy, the invariant cross section plot for alpha particles at 95 A.MeV clearly displays two separated sources for the lowest multiplicity slice (Fig.5a). Notice the rapidity range of the fast source for the most dissipative collisions. Otherwise the IMF velocity distribution presents a main peak below the center of mass velocity associated with a TLF residue on the one hand and a secondary bump around the projectile velocity on the other hand (Fig.5b). Therefore the remaining fragment comes from a binary reaction in which one of the partners has been completely disintegrated in light particles. For light systems in central collisions, Landau-Vlasov calculations predict a final binary behaviour at high incident energy owing to a transparency effect [11].

The 2-IMF events which belong to the most probable partition allow to precise the contribution of binary mechanisms to the total cross section. As previously, multiplicity slices have been used to estimate the centrality of the collisions. Fig.6a displays at 32 A.MeV the relative velocity (V_R) of the two detected fragments versus their parallel velocities. At high V_R, both partners of a binary reaction are clearly

seen : respectively the TLF residue peaked at low parallel velocity and the PLF residue with a range of high velocity. The relative angle (Θ_R) is defined as the angle between the relative velocity and the beam axis. As V_R decreases, Θ_R increases which is interpreted in terms of increasing dissipation (Fig.6b). The arrow on the vertical axis indicates the Coulomb velocity corresponding to completely damped reactions which are observed beyond 50°. The similar behaviour is obtained for the high multiplicity slice with larger dissipation. At last, the strong correlation between the deflection angle and the relative velocity is in good agreement with a deep inelastic process [10].

5 Conclusion

In the Ar+Ni system, the evolution of IMF distributions from 32 to 95 A.MeV has shown that the probability to have a given IMF multiplicity is almost independent of the available energy. On the other hand, the analysis of reaction mechanisms for complete events with 1 and 2-IMF in central collision underlines the dominance of binary dissipative reactions. In this way, a weak cross section for fusion has been measured at 32 A.MeV. Future analysis will be dedicated to a sensitive determination of the primary sources in order to obtain an event classification for the study of hot nuclei de-excitation.

References

[1] B. Borderie, Ann. de Phys. 17 (1992) 349.

[2] L.G. Moretto, G.J. Wozniak, Ann. Rev. Nucl. Part. Sci. 43 (1993) 379.

[3] J. Cugnon, Phys. Lett. B135 (1984) 374.

[4] E. Suraud et al., Nucl. Phys. A495 (1989) 73c;
E. Suraud et al., Phys. Lett. B229 (1989) 359.

[5] J. Bondorf et al., Nucl. Phys. A443 (1985) 321;
J. Bondorf et al., Nucl. Phys. A444 (1985) 460.

[6] J. Pouthas et al., to be published in Nucl. Inst. and Meth.

[7] D.H.E. Gross et al., Rep. Prog. Phys. 53 (1990) 605.

[8] Ch.O. Bacri et al., submitted to Phys. Lett. B.

[9] M.F. Rivet et al., Phys. Lett. B215 (1988) 55.

[10] M. Lefort, C. Ngô, Ann. de Phys. 3 (1978) 5.

[11] V. de la Mota et al., Phys. Rev. C46 (1992) 677.

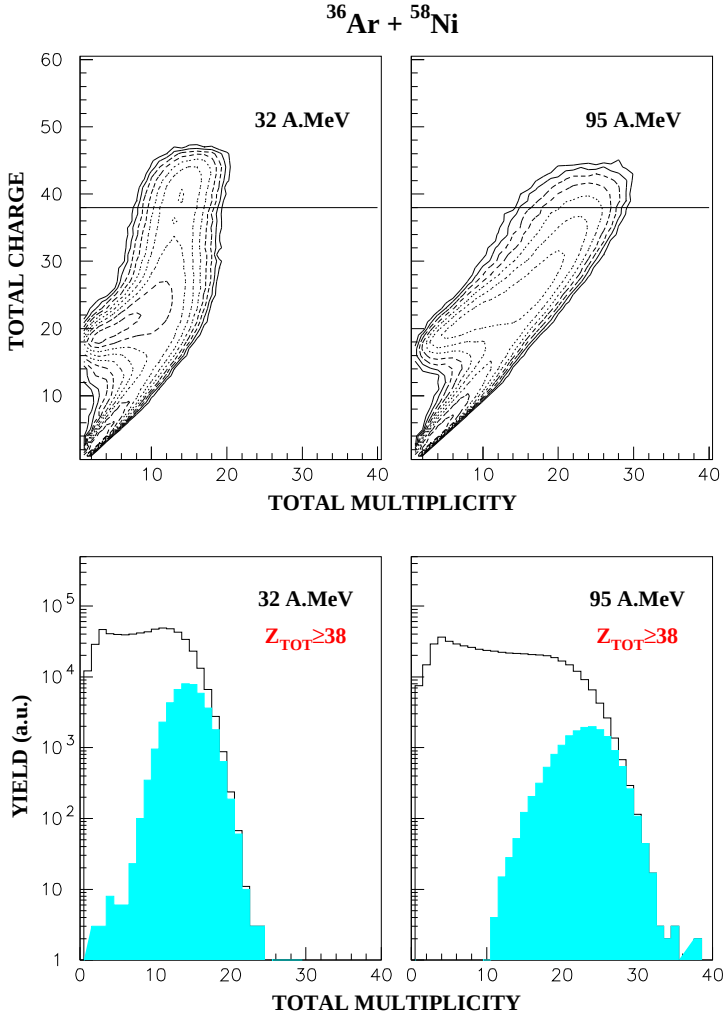

Figure 1: a) Top : Total detected charge as a function of charged particle multiplicity at 32 and 95 A.MeV. The solid line (Z_{TOT}=38) indicates the selection for complete events (80% of the total charge of the system). b) Bottom : Multiplicity distributions for all events (black curve) and complete events (dark area).

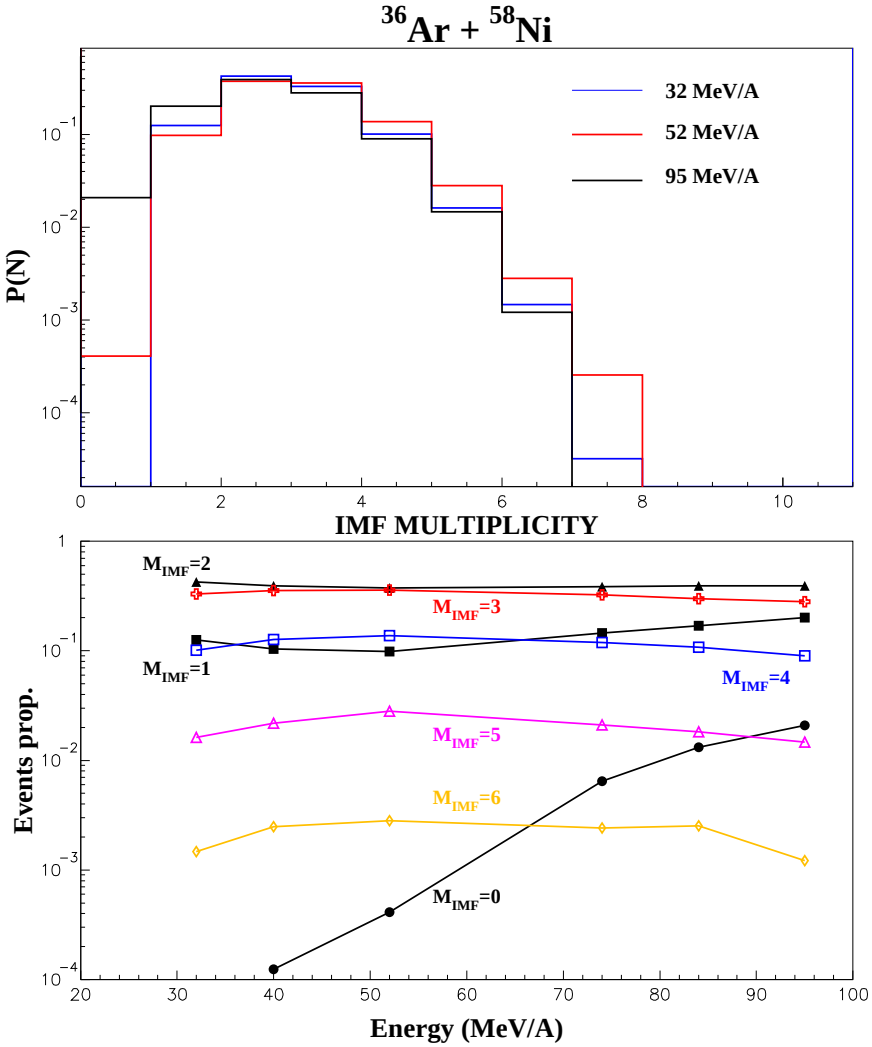

Figure 2: a) Top : IMF normalized distributions at 32, 52 and 95 A.MeV. b) Bottom : Evolution of the IMF partitions with the bombarding energy.

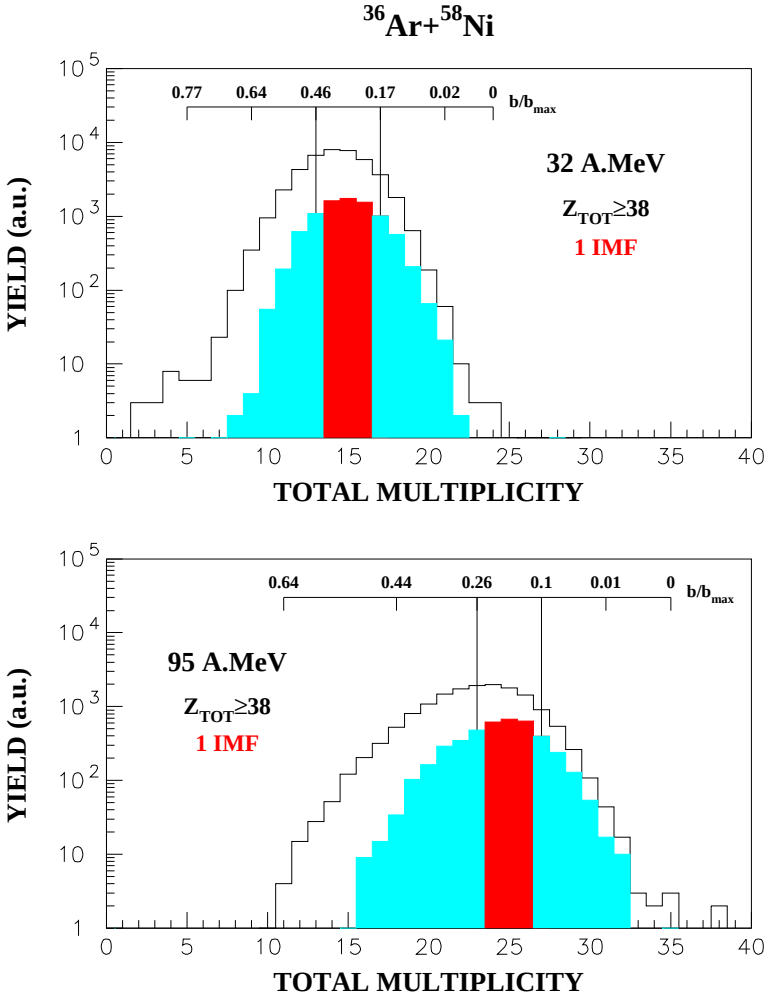

Figure 3: Multiplicity distributions for complete events with 1-IMF at 32 and 95 A.MeV. Each distribution is divided in three multiplicity slices (dark areas). The upper scale gives a reduced impact parameter range (b_{max} ~10 fm).

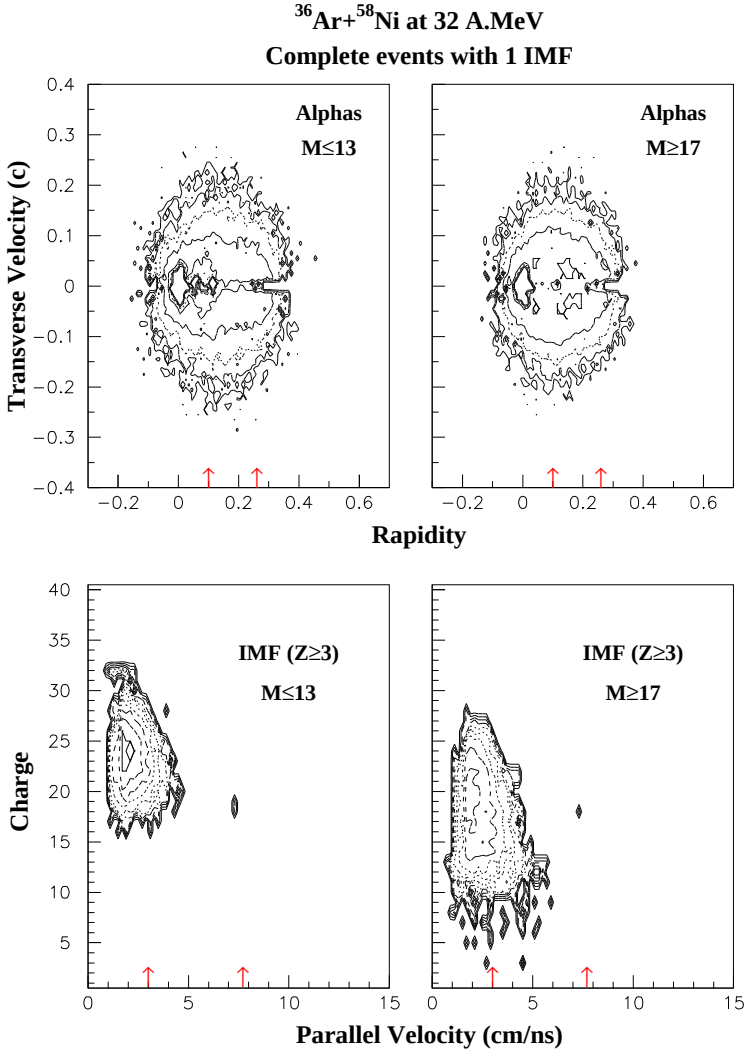

Figure 4: a) Top : Lorentz invariant cross section in the transverse velocity versus rapidity plane for alpha particles associated to the 1-IMF events at 32 A.MeV for the lowest multiplicity slice and the highest one. b) Bottom : Charge versus parallel velocity distributions of the IMF (extreme multiplicity slices). Arrows on the horizontal axis indicate respectively the center of mass and the projectile rapidity (or velocity).

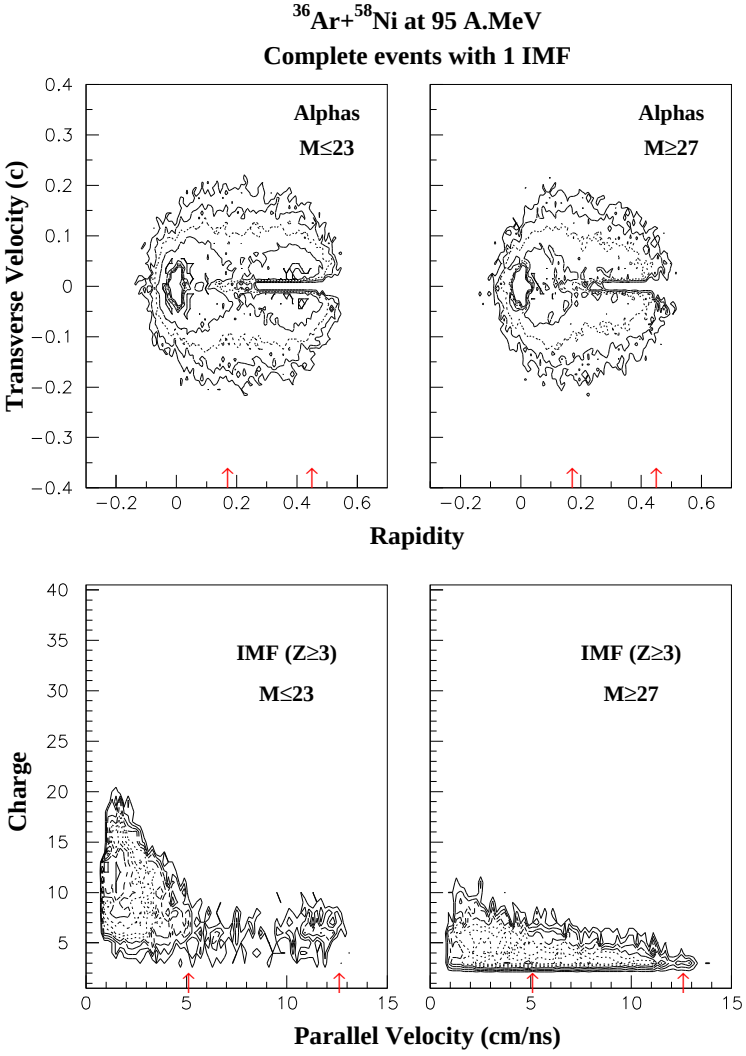

Figure 5: a) Top : Lorentz invariant cross section for alpha particles associated to the 1-IMF events at 95 A.MeV (extreme multiplicity slices). b) Bottom : Charge versus parallel velocity distributions of the IMF (extreme multiplicity slices).

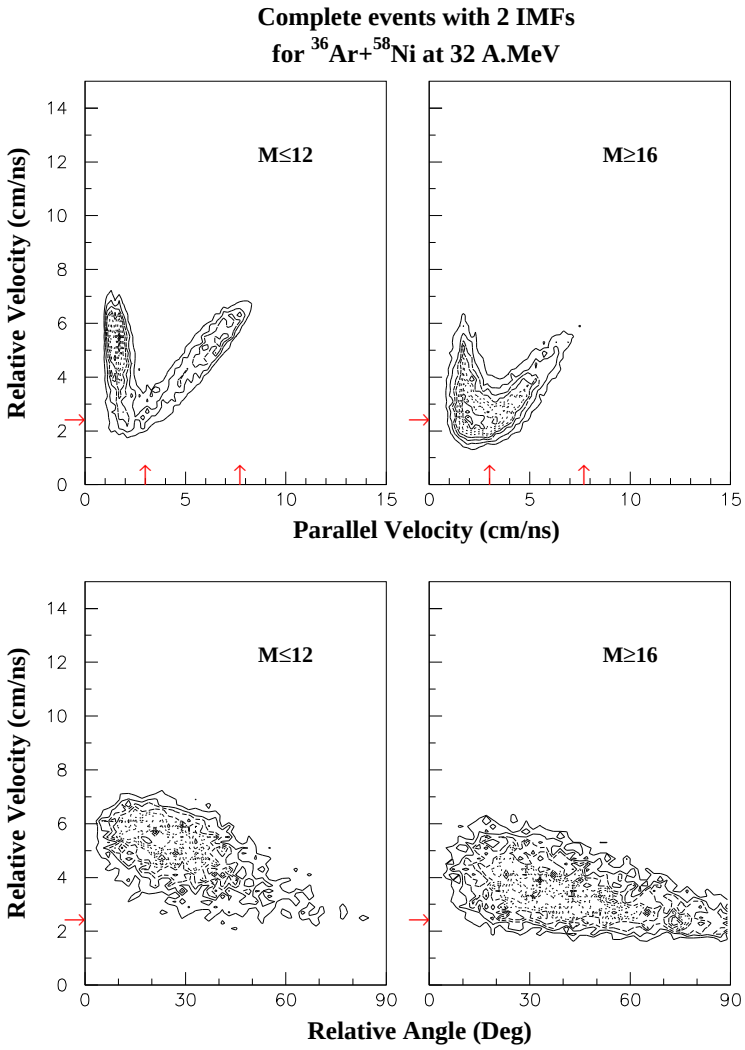

Figure 6: a) Top : Relative velocity between the two IMF as a function of their parallel velocity for the 2-IMF events at 32 A.MeV (extreme multiplicity slices). b) Bottom : IMF relative velocity as a function of the deflection angle (extreme multiplicity slices). Arrow on the vertical axis indicates the Coulomb velocity (damped reactions).